Elsevier Editorial System(tm) for European Journal of Medicinal Chemistry
Manuscript Draft

Manuscript Number: EJMECH-D-14-01857

Title: (Z)-3-(2-(4-arylthiazol-2-yl)hydrazono)indolin-2-one derivatives as dual inhibitors of HIV-1 Reverse Transcriptase

Article Type: Research Paper

Keywords: Antiviral agents, HIV-1 RT dual inhibitors, HIV-1, molecular modelling, RNase H, (Z)-3-(2-(4-arylthiazol-2-yl)hydrazono)indolin-2-ones

Corresponding Author: Prof Elias Maccioni, PhD

Corresponding Author's Institution: University of Cagliari

First Author: Rita Meleddu, PhD

Order of Authors: Rita Meleddu, PhD; Simona Distinto, PhD; Angela Corona, PhD; Giulia Bianco; Valeria Cannas; Francesca Esposito, PhD; Anna Artese, PhD; Stefano Alcaro, PhD; Peter Matyus, PhD; Dora Bogdand; Filippo Cottiglia, PhD; Enzo Tramontano, PhD; Elias Maccioni, PhD

Abstract: The HIV-1 Reverse Transcriptase (RT) is a validated and deeply explored biological target for the treatment of AIDS. However, only drugs targeting the RT-associated DNA polymerase (DP) function have been approved for clinical use. We designed and synthesised a new generation of HIV-1 RT inhibitors, based on the (Z)-3-(2-(4-arylthiazol-2-yl)hydrazono)indolin-2-one scaffold. These compounds are active towards both RT-associated functions, DNA polymerase and ribonuclease H. The structure, biological activity and mode of action of the new derivatives have been investigated. In particular, the nature of the aromatic group in the position 4 of the thiazole ring plays a key role in the modulation of the activity towards the two RT-associated functions.

Title

(*Z*)-3-(2-(4-arylthiazol-2-yl)hydrazono)indolin-2-one derivatives as dual inhibitors of HIV-1 Reverse Transcriptase

Authors

Rita Meleddu[a], Simona Distinto[a], Angela Corona[b], Giulia Bianco[a], Valeria Cannas[a], Francesca Esposito[b], Anna Artese[c], Stefano Alcaro[c], Peter Matyus[d], Dora Bogdand[d], Filippo Cottiglia[a], Enzo Tramontano[b], Elias Maccioni[a*].

Affiliations

[a]Department of Life and Environmental Sciences, University of Cagliari, Via Ospedale 72, 09124 Cagliari, Italy

[b]Department of Life and Environmental Sciences, University of Cagliari, Cittadella Universitaria di Monserrato, SS554, 09042 Monserrato, Cagliari, Italy

[c]Dipartimento di Scienze della Salute, Università Magna Graecia di Catanzaro, Campus "S. Venuta", Viale Europa, 88100 Catanzaro, Italy

[d]Department of Organic Chemistry, Hogyes Endre utca 7, 1092, Semmelweis University, Budapest, Hungary

*To whom correspondence should be addressed. S.D, Department of Life and Environmental Sciences, University of Cagliari, Via Ospedale 72, 09124 Cagliari, Italy; Tel: +39 0706758550; Fax +39 0706758553, E-mail: maccione@unica.it.

Abstract

The HIV-1 Reverse Transcriptase (RT) is a validated and deeply explored biological target for the treatment of AIDS. However, only drugs targeting the RT-associated DNA polymerase (DP) function have been approved for clinical use. We designed and synthesised a new generation of HIV-1 RT inhibitors, based on the (*Z*)-3-(2-(4-arylthiazol-2-yl)hydrazono)indolin-2-one scaffold. These compounds are active towards both RT-associated functions, DNA polymerase and ribonuclease H. The structure, biological activity and mode of action of the new derivatives have been investigated. In particular, the nature of the aromatic group in the position 4 of the thiazole ring plays a key role in the modulation of the activity towards the two RT-associated functions.

Keywords: Antiviral agents, HIV-1 RT dual inhibitors, HIV-1, molecular modelling, RNase H, (*Z*)-3-(2-(4-arylthiazol-2-yl)hydrazono)indolin-2-ones

Abbreviations

HIV-1, Human Immunodeficiency Virus type; HAART, Highly Active Antiretroviral Therapy; RTIs, RT inhibitors; NRTIs/NtRTIs, Nucleoside/Nucleotide RTIs; NNRTI Non-Nucleoside RTIs; DP, DNA polymerase; RNase H, ribonuclease H; RHIs, RNase H inhibitors; NNRTIBP, NNRTIs binding pocket; PLK4, polo-like kinase 4; BACE1, Beta-secretase 1; CRTH2 (DP2), chemoattractant receptor-homologous molecule expressed on Th2 cells (D2 prostanoid receptor); NOE, Nuclear Overhauser Effect, NMR, Nuclear Magnetic Resonance; R.T., room temperature; RNase H, Ribonuclease H; MM-GBSA, the molecular mechanics generalized Born/surface area; MMFFs, Merck Molecular Force Field; GB/SA, Generalized Born/Surface Area; Polak-Ribier Coniugate Gradient (PRCG); QPLD Quantum Mechanic-polarized ligand docking.

1. Introduction

The current approved therapy for the treatment of Human Immunodeficiency Virus type 1 (HIV-1) infection is based on the highly active antiretroviral therapy (HAART), that associates a combination of antiviral agents, targeting different steps of the virus replication cycle [1, 2]. This multidrug therapeutic regimen leads to the reduction of the amount of circulating virus, in some cases below the current blood testing techniques detectable level, and allows high control of the infection, reduction of drug resistance occurrence, decrease of mortality and morbidity rates, and an overall improvement of patients quality of life [3]. However, due to the chronic nature of HIV-infection, a lifelong therapy is required and the adherence to treatment as well as the management of drug-related toxicities are issues to deal with.

Although numerous strategies of simplified treatment have been explored in order to further improve patient quality of life while maintaining treatment success, RT inhibitors (RTIs), both Nucleoside/Nucleotide RTIs (NRTIs/NtRTIs) and Non-Nucleoside RTIs (NNRTIs) are always included in the HAART regimen [1, 2], due to the key role of RT in the early phase of the HIV-1 life cycle.

HIV-1 RT catalyses the reverse transcription process which consists of the conversion of a single strand viral RNA into a double strand viral DNA via the formation of a RNA-DNA hybrid. To perform this activity two main catalytic functions are associated in one enzyme, DNA polymerase (DP) and ribonuclease H (RNase H).

However, despite the fact that both functions are validated drug targets, since also RNase H function is essential for the reverse transcription process [4, 5], no inhibitors, specific for this enzymatic activity, have been introduced in therapy until now [6, 7].

Most RNase H inhibitors (RHIs), designed and studied so far, act by chelating the Mg^{2+} ions within the active site [8-15]. However other mechanisms of action have been reported for hydrazone [16], naphthyridinone [17], anthraquinone [18] and propenone [19] derivatives.

The latter compounds are capable of binding an allosteric pocket close to the NNRTIs binding pocket (NNRTIBP) and of inhibiting the RNase H function by a long range allosteric effect.

We have recently reported the identification of a new scaffold for dual inhibition of both HIV-1 RT-associated RNase H and DP functions [20]. Among all the identified molecules, compound **1** (3Z)-3-(2-[4-(3,4-dihydroxyphenyl)-1,3-thiazol-2-yl]hydrazin-1-ylidene)-2,3-dihydro-1H-indol-2-one (Figure 1) resulted as the best performing derivative with IC_{50} values in the low micromolar range [20].

Firstly, to gain insights into the drug novelty potential of compound **1**, we wanted to investigate its mode of action by measuring its capability to chelate Mg^{2+} ions, since inhibitors which act on the RNase H active site have been reported to chelate the Mg^{2+} [21]. Secondly, we examined if cross resistance with NNRTI resistant RTs could be observed for compound **1**, since this behaviour has been reported for those compounds that interact with the allosteric RNase H pocket, close to the NNRTIBP [16, 18, 22]. Results showed that compound **1** did not chelate Mg^{2+} (Figure 2), but its activity was slightly affected when tested on the Lys103Asn and Tyr181Cys RTs, two NNRTI resistant mutant enzymes [20]. These results suggested that compound **1** could have a mode of action similar to some hydrazone derivatives previously reported [16, 17]. Hence, we performed biochemical and docking experiments that, in agreement with the biochemical data, indicated compound **1** able to bind to RT in the region indicated by Himmel et al in previous works [16, 17]. Therefore, in order to investigate the influence of structural modifications on the biological activity of compound **1**, we synthesised a small library of (3Z)-3-(2-[4-aryl)-1,3-thiazol-2-yl]hydrazin-1-ylidene)-2,3-dihydro-1H-indol-2-ones.

As in the original compound **1**, we have conserved the indolinone and thiazole moieties that have been reported as important fragments in a number of bioactive molecules, such as selective chymase inhibitors [23], polo-like kinase 4 (PLK4) inhibitors [24], Beta-secretase 1 (BACE1) inhibitors [25], chemoattractant receptor-homologous molecule expressed on Th2 cells (D2 prostanoid receptor) (CRTH2 (DP2)) antagonists [26], MAO inhibitors [27] anti-mycobacterial [28,

29], anti-Candida [30], and antimicrobial [31]. In the present work, we introduced differently substituted phenyl moieties at the position 4 of the thiazole in place of the 3,4-dihydroxyphenyl group and evaluated their ability to behave as dual RT-associated functions inhibitors (Figure 1).

Figure 1 here

2. Chemistry

(3Z)-3-(2-[4-aryl)-1,3-thiazol-2-yl]hydrazin-1-ylidene)-2,3-dihydro-1H-indol-2-ones (**EMAC2072-2082**) were synthesized starting from 2,3-dihydro-1H-indole-2,3-dione (I). This was reacted with thiosemicarbazide (II) in 2-propanol to give 2-oxo-2,3-dihydro-1H-indol-3-thiosemicarbazone (III). Equimolar amounts of III and of the appropriate α-halogeno-arylketone (IV) were then stirred in 2-propanol to give the desired final compounds, as depicted in Scheme 1.

Scheme 1 here

All compounds were characterised by means of both analytical and spectroscopic methods. Their analytical and spectroscopic properties are reported in Table S1-S2.

The possible formation of both *E* and *Z* diastereoisomers along the C=N double bond was investigated by Nuclear Overhauser Effect (NOE) experiments.

In each compound, irradiation of the indole CH-4, intensity of the neighbouring CH protons was only changed, whereas upon irradiation of the hydrazone NH signal, there was observed no intensity change. This distance confirm "*Z*". Therefore, *Z*-configuration of each compound could be confirmed (Figure S1). For all the synthesised compounds the *Z* configuration was supported by Nuclear Magnetic Resonance (NMR).

3. Results and discussion

All the synthesised compounds, **EMAC2072-2082**, were evaluated for their ability to inhibit both HIV-1 RT associated RNase H and DP functions (Table 1) using compound **1** as reference control.

Table1 here

All tested compounds, with the exception of compound **EMAC2081**, exhibited dual inhibitory activity towards both HIV-1 RT functions, confirming that the (*Z*)-3-(2-(4-arylthiazol-2-yl)hydrazono)indolin-2-one scaffold could be considered a promising candidate for the design of HIV-1 RT dual functions inhibitor [20]. Interestingly, while compound **1** showed a specificity index (SpI), expressed as the ratio of the RNase H IC_{50} value *versus* the DP IC_{50} value, favourable to the DP function (SpI = 3,5), all derivatives exhibited a SpI favourable to the RNase H function. These results demonstrate that the compounds activity and specificity on the two functions is strongly influenced by the presence and nature of substituents in the 4-phenylthiazole system.

In fact, in the case of compound **EMAC2081**, bearing the un-substituted 4-phenylthiazole moiety, almost no activity towards both functions was observed. Conversely, the introduction of a 4-(4-biphenyl)thiazole moiety (**EMAC2076**) led to one of the most potent compounds, with a SpI of 0.11. However, the introduction of a 4-(3-nitrophenyl)thiazole (**EMAC2078**) appears as the most performing substitution with respect to DP and RNase H inhibition. Instead, the introduction of the 2,4-difluorophenyl thiazole (**EMAC2077**) or the 4-(4-biphenyl)thiazole (**EMAC2076**) is effective towards the RNase H inhibition. Therefore, a mixture of steric and electronic effects should be blended in order to achieve the best activity towards the two RT associated functions. Moreover, the double substitution with halogen atoms in the positions 2 and 4 of the 4-phenyl thiazole is also effective with respect to the mono-substitution. Thus, compounds **EMAC2072** and **EMAC2073** are less potent than their di-substituted analogues **EMAC2082** and **EMAC2077**.

In this respect, fluorine demonstrated to be more efficient than chlorine, probably due to the higher capability to act as hydrogen bond acceptor. Indeed the size of fluorine is intermediate between that of hydrogen and oxygen and its van der Waals radius (1.47 Å) could be compared to those of hydrogen (1.2 Å) and oxygen (1.57 Å). As a matter of fact, we have observed that small changes in structure have dramatic effects on activity.

Dual activity might originate from a set of ligand-enzyme interactions, such as the formation of complexes between the ligand and the NNRTIBP, the RNase H allosteric site, and the RNase H catalytic site. Therefore, a mode of action investigation by means of biochemical and computational methods was performed, in order to identify the mechanism of action and the most probable binding modes of these compounds.

Firstly, we verified the possibility that, differently from compound **1**, EMAC derivatives could bind the RNase H catalytic site through an interaction with the Mg^{2+} ions, measuring their spectrum of absorbance in the absence and in the presence of $MgCl_2$, observing no differences (Figure 2). Hence, it is possible to assume that EMAC derivatives do not inhibit the RNase H function by binding the Mg^{2+} ions in the catalytic site.

Figure 2 here

Next, we investigated the possible binding of EMAC compounds either in the NNRTIBP or in the RNase H allosteric site close to the NNRTIBP. Thus the effects of **EMAC2076** on Tyr181Cys and Lys103Asn mutated RT, involved in NNRTI resistance [32], were evaluated using the NNRTI Efavirenz and the DKA **RDS1643** as controls (Table 2). Results showed that **EMAC2076** retains its potency of inhibition of both RT-associated functions when tested on Lys103Asn and Tyr181Cys RTs. Its behaviour is analogue to that previously reported of compound **1**: mutated residues were not essential for the interaction of inhibitor with the HIV-1 RT. Therefore EMAC derivatives are promising hit candidates considering that their activity is not affected when assayed on common resistant mutants.

Table 2 here

To study the binding mode of compound **EMAC2076** with RT HIV-1, docking experiments were performed considering the same protocol described in the previous work [20]. The allosteric RNase H binding pocket of RT is mainly lipophilic with aromatic residues, and therefore hydrophobic interactions play crucial role on determining anti-HIV activity, and it is characterized by an L shape expanding from the region next to catalytic DP site to the NNRTIBP [33].

The obtained [**EMAC2076**•RT] complexes were subjected to a post-docking procedure based on energy minimization and subsequent binding free energies calculation. The free energies of binding were obtained applying molecular mechanics and continuum solvation models using the molecular mechanics Generalized Born/Surface Area (MM-GBSA) method [34].

To further validate the docking pose, the experiment was carried out also on Tyr181Cys mutated enzyme. The best docking poses (Figure 3) show that Tyr181Cys mutation did not change the ligand binding mode.

Moreover, the evaluated energies of interaction are comparable (-43.87 *vs* -42.89 kcal/mol). This is in agreement with the biological data.

The best docking pose for **EMAC2076** shows the molecule interested by Van-der-Waals contacts with Leu228, Val108, Pro226 side-chains. The biphenyl substituent is oriented towards NNRTIBP and stabilized by an array of aromatic π–π interactions involving Tyr188, Phe227 and Trp229. However, the rigidity of this group does not allow the compound to enter more deeply in the L pocket. Stacking contacts are also possible with Tyr181Cys mutation, which was shown to confer no resistance to this inhibitor (Table 2). Interestingly, the biphenyl hydrophobic substituent orients the compound with the indolinone portion outside the pocket, while the previously reported compound **1** seems to prefer an orientation rotated of 180°. A possible explanation is given by the presence of the more polar di-hydroxyphenyl moiety in compound **1** with respect to the lipophilic biphenyl substituent of compound **EMAC2076**. Such polar substituent confers a higher water affinity flipping the ligand with the thiazole portion oriented to the outer, solvent exposed, part of the enzyme cavity. Furthermore, this orientation is stabilised through a favourable π–π stacking between indolinone portion and Trp229. However, in our opinion, the binding mode of **EMAC2076** offers more space for chemical optimization, since the activity of these derivatives could be further improved with a wide variety of hydrophobic and heterocyclic substituents in position 4 of thiazole ring and by keeping the indolinone portion oriented towards the solvent. Indeed, it seems important

to maintain an aromatic moiety to allow stacking interactions with the conserved residues Phe227 and Trp229, lining in this-binding pocket [35].

On the whole, the good agreement between the drug resistance mutation profile and the docking poses represents a further validation of the obtained results.

Figure 3 here

4. Conclusion

The present study describes a simple method for the synthesis of indolinone derivatives. These compounds show interesting dual inhibitory activity on both RNase H and DP HIV-1 RT-associated functions, leading to inhibitors that may completely block RT activities. These compounds seem to be able to bind a protein allosteric pocket that modulates both RT activities. Furthermore, the most active compound shows a favourable drug resistance profile. Since the system seems really susceptible to aromatic substituents in position 4 of thiazole, the activity could be further improved with a wide variety of substituents, and heterocyclic systems and through an accurate modulation of electronic, steric and solvation effects. These new derivatives could be considered as a key step towards the design of dual DP/RNase H HIV 1 RT inhibitors.

5. Experimental Section

5.1 Material and General methods

Starting materials and reagents were obtained from commercial suppliers and were used without purification. All melting points were determined by the capillary method on a Büchi-540 capillary melting points apparatus and are uncorrected. Melting points, yield of reactions and the analytical data of derivatives are reported respectively in Tables S1 and S2 of SD.

All samples were measured in DMF-d_7 or DMSO-d_6 solvent at 278.1 K temperature on a Bruker AVANCE III 500 MHz spectrometer. Chemical shifts are reported relative to TMS ($\delta = 0$) and/or referenced to the solvent in which they were measured. (In the ^{15}N chemical shift assignments we

applied the spectrometer's digital reference which is calibrated to liq. NH3 δ = 0 ppm.) Coupling constants *J* are expressed in hertz (Hz).

Elemental analyses were obtained on a Perkin–Elmer 240 B microanalyser. Analytical data of the synthesised compounds are in agreement within ± 0.4 % of the theoretical values. TLC chromatography was performed using silica gel plates (Merck F 254), spots were visualised by UV light.

***5.1.2 NMR Compounds characterisation**:*

*5.1.2.1 (Z)-3-(2-(4-(4-chlorophenyl)thiazol-2-yl)hydrazono)indolin-2-one (**EMAC2072**)*

^{1}H NMR (DMF) δ(ppm): 13.55 (s, 1H); 11.43 (s; 1H); 8.07-8.02 (m; 2H); 7.82 (s; 1H); 7.63 (dm; J=7.6 Hz; 1H); 7.58-7.53 (m; 2H); 7.41 (td; J=7.6 Hz; 1.1 Hz; 1H); 7.16 (td; J=7.6 Hz; 1.0 Hz; 1H); 7.10 (dm; J=7.6 Hz; 1H)

^{13}C NMR (DMF) δ(ppm): 166.9; 164.0; 150.6; 142.1; 133.6; 133.1; 132.7; 130.9; 129.2; 127.9; 122.8; 120.5; 120.3; 111.5; 107.7

^{15}N NMR (DMF) δ(ppm): 156.2; 135.7

*5.1.2.2 (Z)-3-(2-(4-(4-fluorophenyl)thiazol-2-yl)hydrazono)indolin-2-one (**EMAC2073**)*

^{1}H NMR (DMSO) δ(ppm): 13.33 (s; 1H); 11.25 (s; 1H); 7.97-7.90 (m; 2H); 7.60 (s; 1H); 7.53 (dm; J= 7.5 Hz; 1H); 7.34 (tm; J= 7.5 Hz; 1H); 7.29-7.17 (m; 2H); 7.09 (tm; J= 7.5 Hz; 1H); 6.99-6.92 (m; 1H)

^{13}C NMR (DMSO) δ(ppm): 166.4; 163.2; 161.9 (d; J= 244.6 Hz); 150.0; 141.3; 132.2; 130.6; 130.5; 127.8 (d; J= 8.3 Hz) 122.4; 119.9; 119.8; 115.6 (d; J= 21.6 Hz); 111.1; 106.6

^{15}N NMR (DMSO) δ(ppm): 137.1

*5.1.2.3 (Z)-3-(2-(4-(4-bromophenyl)thiazol-2-yl)hydrazono)indolin-2-one (**EMAC2074**)*

^{1}H NMR (DMF) δ(ppm): 13.53 (s; 1H); 11.42 (s; 1H); 7.99-7.93 (m; 2H); 7.82 (s; 1H); 7.71-7.65 (m; 2H); 7.61 (dm; J= 7.6 Hz; 1H); 7.39 (tm; J= 7.6 Hz; 1H); 7.14 (tm; J= 7.6 Hz; 1H); 7.08 (dm; J= 7.6 Hz; 1H)

^{13}C NMR (DMF) δ(ppm): 167.0; 164.0; 150.7; 142.1; 133.9; 132.7; 132.1; 130.9; 128.1; 122.8; 121.6; 120.5; 120.3; 111.5; 107.8

^{15}N NMR (DMF) δ(ppm): 156.1; 135.7

*5.1.2.4 (Z)-3-(2-(4-(4-nitrophenyl)thiazol-2-yl)hydrazono)indolin-2-one (**EMAC2075**)*

^{1}H NMR (DMF) δ(ppm): 13.55 (s; 1H); 11.42 (s;1H); 8.38-8.32 (m; 2H); 8.30-8.24 (m; 2H); 8.12 (s; 1H); 7.62 (dm; J= 7.7 Hz; 1H); 7.40 (td; J= 7.7 Hz; 1.2 Hz; 1H); 7.15 (td; J= 7.7 Hz; 0.7 Hz; 1H); 7.08 (dm; J= 7.7 Hz; 1H)

^{13}C NMR (DMF) δ(ppm): 167.3; 163.9; 149.7; 147.2; 142.2; 140.7; 133.1; 131.1; 127.0; 124.5; 122.9; 120.4; 120.3; 111.6; 111.6

^{15}N NMR (DMF) δ(ppm): 155.8; 135.7

5.1.2.5 (Z)-3-{2-[4-(4-biphenyl)- thiazol-2-yl)hydrazono)indolin-2-one (***EMAC2076***)

^{1}H NMR (DMF) δ(ppm): 13.56 (s; 1H); 11.41 (s; 1H); 8.13-8.08 (m; 2H); 7.85-7.75 (m; 5H); 7.63 (d; *J*= 7.6 Hz; 1H); 7.55-7.49 (m; 2H); 7.44-7.36 (m; 2H); 7.15 (tm; *J*= 7.6 Hz; 1H); 7.08 (dm; *J*= 7.6 Hz; 1H)

^{13}C NMR (DMF) δ(ppm): 166.8; 164.0; 151.6; 142.1; 140.4; 140.3; 133.8; 132.6; 130.9; 129.4; 127.9; 127.4; 127.0; 126.7; 122.8; 120.5; 120.2; 111.5; 107.1

^{15}N NMR (DMF) δ(ppm): 156.5; 135.7

*5.1.2.6 (Z)-3-(2-(4-(2,4-difluorophenyl)thiazol-2-yl)hydrazono)indolin-2-one (**EMAC2077**)*

^{1}H NMR (DMF) δ(ppm): 13.52 (s; 1H); 11.39 (s; 1H); 8.23-8.14 (m; 1H); 7.62 (d; J= 7.6 Hz; 1H); 7.58(d; J= 2.4 Hz; 1H); 7.45-7.36 (m; 2H); 7.25 (td; J= 8.5 Hz; 2.5 Hz; 1H); 7.15 (td; J= 7.6 Hz; 0.7 Hz; 1H); 7.07 (dm; J= 7.6 Hz; 1H)

^{13}C NMR (DMF) δ(ppm): 166.4; 164.0; 162.3 (dd; J= 248.0 Hz; 12.4 Hz); 160.4 (dd; J= 251.9 Hz; 12.3 Hz); 144.7 (dd; J= 2.6 Hz; 0.9 Hz); 142.1; 132.8; 131.2 (dd; J= 9.6Hz; 4.8 Hz); 131.0; 122.9; 120.5; 120.3; 119.1 (dd; J= 11.3Hz; 3.7 Hz); 112.3 (dd; J= 21.4Hz; 3.4 Hz); 111.5; 111.2 (d; J= 15.0 Hz); 104.9 (t; J= 26.5 Hz)

^{15}N NMR (DMF) δ(ppm): 155.9; 135.5

*5.1.2.7 (Z)-3-(2-(4-(3-nitrophenyl)thiazol-2-yl)hydrazono)indolin-2-one (**EMAC2078**)*

^{1}H NMR (DMF) δ(ppm): 13.57 (s; 1H); 11.41 (s; 1H); 8.84-8.76 (m; 1H); 8.46 (dm; J= 8.1 Hz; 1H); 8.26 (dm; J= 8.1 Hz; 1H); 8.09 (s; 1H); 7.80 (t; J= 8.1 Hz; 1H); 7.63 (d; J= 7.6 Hz; 1H); 7.41 (tm; J= 7.6 Hz; 1H); 7.15 (tm; J= 7.6 Hz; 1H); 7.08 (dm; J= 7.6 Hz; 1H)

^{13}C NMR (DMF) δ(ppm): 167.3; 164.0; 149.5; 149.0; 142.2; 136.3; 133.0; 132.2; 131.0; 130.7; 122.9; 122.9; 120.6; 120.4; 120.3; 111.5; 109.6

^{15}N NMR (DMF) δ(ppm): 155.9; 135.5

*5.1.2.8 (Z)-3-(2-(4-p-tolylthiazol-2-yl)hydrazono)indolin-2-one (**EMAC2079**)*

^{1}H NMR (DMF) δ(ppm): 13.53 (s; 1H); 11.38 (s; 1H); 7.91-7.86 (m; 2H); 7.66 (s; 1H); 7.62 (d; J= 7.6 Hz; 1H); 7.39 (td; J= 7.6 Hz; 1.2 Hz; 1H); 7.30-7.25 (m; 2H); 7.15 (td; J= 7.6 Hz; 0.8 Hz; 1H); 7.07 (dm; J= 7.6 Hz; 1H); 2.35 (s; 3H)

^{13}C NMR (DMF) δ(ppm): 166.6; 164.0; 152.0; 142.0; 138.0; 132.4; 132.1; 130.8; 129.7; 126.1; 122.8; 120.5; 120.2; 111.5; 106.0; 20.8

^{15}N NMR (DMF) δ(ppm): 156.4; 135.5

*5.1.2.9 (Z)-3-(2-(4-(4-methoxyphenyl)thiazol-2-yl)hydrazono)indolin-2-one (**EMAC2080**)*

^{1}H NMR (DMF) δ(ppm): 13.53 (s; 1H); 11.40 (s; 1H); 7.95-7.91 (m; 2H); 7.63-7.59 (dm; J= 7.7 Hz; 1H); 7.56 (s; 1H); 7.39 (td; J= 7.7 Hz; 1.1 Hz; 1H); 7.15 (td; J= 7.7 Hz; 1.0 Hz; 1H); 7.08 (dm; J= 7.7 Hz; 1H); 7.06-7.02 (m, 2H); 3.85 (s; 3H)

^{13}C NMR (DMF) δ(ppm): 166.6; 164.0; 159.9; 151.8; 142.0; 132.4; 130.8; 127.5; 127.5; 122.8; 120.5; 120.2; 114.3; 111.5; 104.7; 55.3

^{15}N NMR (DMF) δ(ppm): 156.6; 135.6

*5.1.2.10 (Z)-3-(2-(4-phenylthiazol-2-yl)hydrazono)indolin-2-one (**EMAC2081**)*

^{1}H NMR (DMF) δ(ppm): 13.54 (s; 1H); 11.41 (s; 1H); 8.01-7.97 (m; 2H); 7.74 (s; 1H); 7.62 (dm; J= 7.7 Hz; 1H); 7.49-7.44 (m; 2H); 7.42-7.34 (m; 2H); 7.17-7.10 (m; 1H); 7.08 (dm; J= 7.7 Hz; 1H)

^{13}C NMR (DMF) δ(ppm): 166.8; 164.0; 151.9; 142.1; 134.7; 132.6; 130.9; 129.1; 128.3; 126.1; 122.8; 120.5; 120.2; 111.5; 106.9

^{15}N NMR (DMF) δ(ppm): 156.2; 135.6

*5.1.2.11 (Z)-3-(2-(4-(2,4-dichlorophenyl)thiazol-2-yl)hydrazono)indolin-2-one (**EMAC2082**)*

^{1}H NMR (DMF) δ(ppm): 13.51 (s; 1H); 11.39 (s; 1H); 8.05 (d; J= 8.5 Hz; 1H); 7.85 (s; 1H); 7.75 (d; J= 2.2 Hz; 1H); 7.63 (dm; J= 7.6 Hz; 1H); 7.58 (dd; J= 8.5 Hz; 2.2 Hz; 1H); 7.40 (td; J= 7.6 Hz; 1.2 Hz; 1H); 7.15 (td; J= 7.6 Hz; 1.0 Hz; 1H); 7.07 (dm; J= 7.6 Hz; 1H)

^{13}C NMR (DMF) δ(ppm): 166.1; 164.0; 147.1; 142.1; 133.6; 132.6; 132.9; 132.2; 132.1; 131.0; 130.4; 128.1; 122.9; 120.5; 120.3; 112.9; 111.5

^{15}N NMR (DMF) δ(ppm): 155.6; 135.5

5.2 Biochemistry studies

5.2.1 HIV-1 RT purification.

Heterodimeric RT was expressed essentially as described [36].

5.2.2 HIV-1 RT-associated DNA polymerase-independent RNase H activity determination.

The HIV RT-associated RNase H activity was measured as described [37]. Briefly, in 100 µL reaction volume containing 50 mM Tris HCl pH 7.8, 6 mM $MgCl_2$, 1 mM dithiothreitol (DTT), 80 mM KCl, 250nM hybrid RNA/DNA (5'-GTTTTCTTTTCCCCCCTGAC-3'-Fluorescein, 5'-CAAAAGAAAAGGGGGGACUG-3'-Dabcyl) and 20 ng of wt RT. The reaction mixture was incubated for 1 h at 37 °C, the reaction was stopped by addition of EDTA and products were measured with a Victor 3 (Perkin) at 490/528 nm.

5.2.3 HIV-1 RT-associated RNA dependent DNA polymerase activity determination.

The HIV-1 RT-associated RNA-Dependent DP activity was measured as previously described [38]. Briefly, in 25 µL volume containing 60 mM Tris-HCl pH 8.1, 8 mM $MgCl_2$, 60 mM KCl, 13 mM DTT, 2.5 µM poly(A)-oligo(dT), 100 µM dTTP and 20 ng of wt RT. After enzyme addition, the reaction mixture was incubated for 30 min at 37 °C and enzymatic reaction was stopped by addition of EDTA. Reaction products were detected by picogreen addition and measured with a Victor 3 (Perkin) at 502/523 nm.

5.3 Molecular Modeling

5.3.1 Ligand preparation.

The ligand was built within Maestro GUI and its geometry was optimized. The lowest energy conformer was considered for the following studies. This was obtained with MacroModel version 7.2 [39], considering MMFFs [40] as force field and solvent effects by adopting the implicit solvation model Generalized Born/Surface Area (GB/SA) water [41]. The simulation was performed allowing 1000 steps Monte Carlo analysis with Polak-Ribier Coniugate Gradient (PRCG) method and a convergence criterion of 0.05 kcal/(molÅ).

5.3.2. Protein Preparation.

The atomic coordinates of the protein with pdb code 3LP2 [17] were imported into the Maestro module available in the Schrödinger package[42]. The protein was further optimized using the Protein Preparation Wizard[42].

5.3.3 Docking and post-docking procedure.

The docking experiments were performed as described in our previous work [20] applying Quantum Mechanic-polarized ligand docking (QPLD) [43]. In order to better take into account the induced fit phenomena, the most energy favoured generated complexes were fully optimized with the AMBER* united atoms force field [44] in GB/SA implicit water [41], setting 10000 steps iteractions analysis with Polak-Ribier Coniugate Gradient (PRCG) method and a convergence criterion of 0.1 kcal/(molÅ). Analysis of the results of the complex minimization was carried out taking into account the state equations (free energy of complex formation) computed at 300 K, applying molecular mechanics and continuum solvation models with the molecular mechanics generalized Born [34]. The resulting complexes were considered for the binding modes graphical analysis with Pymol [45] and Maestro [42].

Acknowledgements

This work was supported by RAS grant LR 7/2007 CRP2_450, CRP-24915, and Istituto Superiore di Sanità grant RF-PAD-2009-1304305 n. 40H98. Rita Meleddu PhD grant was founded by Fondazione Banco di Sardegna.

Appendix. Supplementary material

Supplementary material associated with this article: NOE effect for E and Z configuration; chemical and physical data and analytical data of derivatives **EMAC2072-2082.** Supplementary material associated with this article can be found, in the online version, at...

References

[1] P. Zhan, X. Liu, Z. Li, C. Pannecouque, E. De Clercq, Design strategies of novel NNRTIs to overcome drug resistance, Curr. Med. Chem., 16 (2009) 3903-3917.

[2] R. Morphy, Z. Rankovic, Designed multiple ligands. An emerging drug discovery paradigm, J. Med. Chem., 48 (2005) 6523-6543.

[3] M.S. Hirsch, Initiating Therapy: When to Start, What to Use, J. Infect. Dis., 197 (2008) S252-S260.

[4] E. Tramontano, HIV-1 RNase H: recent progress in an exciting, yet little explored, drug target, Mini Rev. Med. Chem., 6 (2006) 727-737.

[5] K. Klumpp, T. Mirzadegan, Recent progress in the design of small molecule inhibitors of HIV RNase H, Curr. Pharm. Des., 12 (2006) 1909-1922.

[6] A. Corona, F. Esposito, E. Tramontano, Can the ever-promising target HIV reverse transcriptase-associated RNase H become a success story for drug development?, Future Vir., 9 (2014) 445-448.

[7] A. Corona, T. Masaoka, G. Tocco, E. Tramontano, S.F.J. Le Grice, Active site and allosteric inhibitors of the ribonuclease H activity of HIV reverse transcriptase, Future Med. Chem., 5 (2013) 2127-2139.

[8] D.M. Himmel, K.A. Maegley, T.A. Pauly, J.D. Bauman, K. Das, C. Dharia, A.D. Clark Jr, K. Ryan, M.J. Hickey, R.A. Love, S.H. Hughes, S. Bergqvist, E. Arnold, Structure of HIV-1 Reverse Transcriptase with the Inhibitor β-Thujaplicinol Bound at the RNase H Active Site, Structure, 17 (2009) 1625-1635.

[9] S. Chung, D.M. Himmel, J.-K. Jiang, K. Wojtak, J.D. Bauman, J.W. Rausch, J.A. Wilson, J.A. Beutler, C.J. Thomas, E. Arnold, S.F.J. Le Grice, Synthesis, Activity, and Structural Analysis of Novel α-Hydroxytropolone Inhibitors of Human Immunodeficiency Virus Reverse Transcriptase-Associated Ribonuclease H, J. Med. Chem., 54 (2011) 4462-4473.

[10] T.A. Kirschberg, M. Balakrishnan, N.H. Squires, T. Barnes, K.M. Brendza, X. Chen, E.J. Eisenberg, W. Jin, N. Kutty, S. Leavitt, A. Liclican, Q. Liu, X. Liu, J. Mak, J.K. Perry, M. Wang, W.J. Watkins, E.B. Lansdon, RNase H Active Site Inhibitors of Human Immunodeficiency Virus

Type 1 Reverse Transcriptase: Design, Biochemical Activity, and Structural Information, J. Med. Chem., 52 (2009) 5781-5784.

[11] E.B. Lansdon, Q. Liu, S.A. Leavitt, M. Balakrishnan, J.K. Perry, C. Lancaster-Moyer, N. Kutty, X. Liu, N.H. Squires, W.J. Watkins, T.A. Kirschberg, Structural and Binding Analysis of Pyrimidinol Carboxylic Acid and N-Hydroxy Quinazolinedione HIV-1 RNase H Inhibitors, Antimicrob. Agents Chemother., 55 (2011) 2905-2915.

[12] J.Q. Hang, S. Rajendran, Y. Yang, Y. Li, P. Wong Kai In, H. Overton, K.E.B. Parkes, N. Cammack, J.A. Martin, K. Klumpp, Activity of the isolated HIV RNase H domain and specific inhibition by N-hydroxyimides, Biochem. Biophys. Res. Commun., 317 (2004) 321-329.

[13] E. Tramontano, F. Esposito, R. Badas, R. Di Santo, R. Costi, P. La Colla, 6-[1-(4-Fluorophenyl)methyl-1H-pyrrol-2-yl)]-2,4-dioxo-5-hexenoic acid ethyl ester a novel diketo acid derivative which selectively inhibits the HIV-1 viral replication in cell culture and the ribonuclease H activity in vitro, Antivir. Res., 65 (2005) 117-124.

[14] R. Costi, M. Métifiot, F. Esposito, G. Cuzzucoli Crucitti, L. Pescatori, A. Messore, L. Scipione, S. Tortorella, L. Zinzula, E. Novellino, Y. Pommier, E. Tramontano, C. Marchand, R. Di Santo, 6-(1-Benzyl-1H-pyrrol-2-yl)-2,4-dioxo-5-hexenoic Acids as Dual Inhibitors of Recombinant HIV-1 Integrase and Ribonuclease H, Synthesized by a Parallel Synthesis Approach, J. Med. Chem., 56 (2013) 8588-8598.

[15] F. Esposito, E. Tramontano, Past and future. Current drugs targeting HIV-1 integrase and reverse transcriptase-associated ribonuclease H activity: single and dual active site inhibitors, Antivir. Chem. Chemother., 23 (2014) 129-144.

[16] D.M. Himmel, S.G. Sarafianos, S. Dharmasena, M.M. Hossain, K. McCoy-Simandle, T. Ilina, A.D. Clark, Jr., J.L. Knight, J.G. Julias, P.K. Clark, K. Krogh-Jespersen, R.M. Levy, S.H. Hughes, M.A. Parniak, E. Arnold, HIV-1 reverse transcriptase structure with RNase H inhibitor dihydroxy benzoyl naphthyl hydrazone bound at a novel site, ACS Chem. Biol., 1 (2006) 702-712.

[17] H.P. Su, Y. Yan, G.S. Prasad, R.F. Smith, C.L. Daniels, P.D. Abeywickrema, J.C. Reid, H.M. Loughran, M. Kornienko, S. Sharma, J.A. Grobler, B. Xu, V. Sardana, T.J. Allison, P.D. Williams, P.L. Darke, D.J. Hazuda, S. Munshi, Structural basis for the inhibition of RNase H activity of HIV-1 reverse transcriptase by RNase H active site-directed inhibitors, J. Virol., 84 (2010) 7625-7633.

[18] F. Esposito, T. Kharlamova, S. Distinto, L. Zinzula, Y.-C. Cheng, G. Dutschman, G. Floris, P. Markt, A. Corona, E. Tramontano, Alizarine derivatives as new dual inhibitors of the HIV-1 reverse transcriptase-associated DNA polymerase and RNase H activities effective also on the RNase H activity of non-nucleoside resistant reverse transcriptases, FEBS J., 278 (2011) 1444-1457.

[19] R. Meleddu, V. Cannas, S. Distinto, G. Sarais, C. DelVecchio, F. Esposito, G. Bianco, A. Corona, F. Cottiglia, S. Alcaro, C. Parolin, A. Artese, D. Scalise, M. Fresta, A. Arridu, F. Ortuso, E. Maccioni, E. Tramontano, Design, synthesis, and biological evaluation of 1,3-diarylpropenones as dual inhibitors of HIV-1 reverse transcriptase, ChemMedChem, 9 (2014) 1869-1879.

[20] S. Distinto, F. Esposito, J. Kirchmair, M.C. Cardia, M. Gaspari, E. Maccioni, S. Alcaro, P. Markt, G. Wolber, L. Zinzula, E. Tramontano, Identification of HIV-1 reverse transcriptase dual inhibitors by a combined shape-, 2D-fingerprint- and pharmacophore-based virtual screening approach, Eur. J. Med. Chem., 50 (2012) 216-229.

[21] E. Tramontano, R. Di Santo, HIV-1 RT-Associated RNase H Function Inhibitors: Recent Advances in Drug Development, Curr. Med. Chem., 17 (2010) 2837-2853.

[22] T. Kharlamova, F. Esposito, L. Zinzula, G. Floris, C. Yung-Chi, G.E. Dutschman, E. Tramontano, Inhibition of HIV-1 ribonuclease H activity by novel frangula-emodine derivatives, Med. Chem., 5 (2009) 398-410.

[23] S.J. Taylor, A.K. Padyana, A. Abeywardane, S. Liang, M.-H. Hao, S. De Lombaert, J. Proudfoot, B.S. Farmer, X. Li, B. Collins, L. Martin, D.R. Albaugh, M. Hill-Drzewi, S.S. Pullen, H. Takahashi, Discovery of Potent, Selective Chymase Inhibitors via Fragment Linking Strategies, J. Med. Chem., 56 (2013) 4465-4481.

[24] R. Laufer, B. Forrest, S.-W. Li, Y. Liu, P. Sampson, L. Edwards, Y. Lang, D.E. Awrey, G. Mao, O. Plotnikova, G. Leung, R. Hodgson, I. Beletskaya, J.M. Mason, X. Luo, X. Wei, Y. Yao, M. Feher, F. Ban, R. Kiarash, E. Green, T.W. Mak, G. Pan, H.W. Pauls, The Discovery of PLK4 Inhibitors: (E)-3-((1H-Indazol-6-yl)methylene)indolin-2-ones as Novel Antiproliferative Agents, J. Med. Chem., 56 (2013) 6069-6087.

[25] J. Yuan, S. Venkatraman, Y. Zheng, B.M. McKeever, L.W. Dillard, S.B. Singh, Structure-Based Design of β-Site APP Cleaving Enzyme 1 (BACE1) Inhibitors for the Treatment of Alzheimer's Disease, J. Med. Chem., 56 (2013) 4156-4180.

[26] S. Crosignani, C. Jorand-Lebrun, P. Page, G. Campbell, V. Colovray, M. Missotten, Y. Humbert, C. Cleva, J.-F. Arrighi, M. Gaudet, Z. Johnson, P. Ferro, A. Chollet, Optimization of the Central Core of Indolinone–Acetic Acid-Based CRTH2 (DP2) Receptor Antagonists, ACS Med. Chem. Lett., 2 (2011) 644-649.

[27] S. Distinto, M. Yáñez, S. Alcaro, M.C. Cardia, M. Gaspari, M.L. Sanna, R. Meleddu, F. Ortuso, J. Kirchmair, P. Markt, A. Bolasco, G. Wolber, D. Secci, E. Maccioni, Synthesis and biological assessment of novel 2-thiazolylhydrazones and computational analysis of their recognition by monoamine oxidase B, Eur. J. Med. Chem., 48 (2012) 284-295.

[28] V.U. Jeankumar, J. Renuka, P. Santosh, V. Soni, J.P. Sridevi, P. Suryadevara, P. Yogeeswari, D. Sriram, Thiazole–aminopiperidine hybrid analogues: Design and synthesis of novel Mycobacterium tuberculosis GyrB inhibitors, Eur. J. Med. Chem., 70 (2013) 143-153.

[29] P. Makam, R. Kankanala, A. Prakash, T. Kannan, 2-(2-Hydrazinyl)thiazole derivatives: Design, synthesis and in vitro antimycobacterial studies, Eur. J. Med. Chem., 69 (2013) 564-576.

[30] F. Chimenti, B. Bizzarri, E. Maccioni, D. Secci, A. Bolasco, R. Fioravanti, P. Chimenti, A. Granese, S. Carradori, D. Rivanera, D. Lilli, A. Zicari, S. Distinto, Synthesis and in vitro activity of 2-thiazolylhydrazone derivatives compared with the activity of clotrimazole against clinical isolates of Candida spp, Bioorg. Med. Chem. Lett., 17 (2007) 4635-4640.

[31] L. Xiaoyun, L. Xiaobo, W. Baojie, G.F. Scott, C. Lili, Z. Changlin, Y. Qidong, Synthesis and Evaluation of Antitubercular and Antibacterial Activities of New 4‐(2,6‐Dichlorobenzyloxy)phenyl Thiazole, Oxazole and Imidazole Derivatives. Part 2, Eur. J. Med. Chem., 49 (2012) 164-171.

[32] Y. Mehellou, E. De Clercq, Twenty-Six Years of Anti-HIV Drug Discovery: Where Do We Stand and Where Do We Go?, J. Med. Chem., 53 (2009) 521-538.

[33] S. Distinto, E. Maccioni, R. Meleddu, A. Corona, S. Alcaro, E. Tramontano, Molecular Aspects of the RT/drug Interactions. Perspective of Dual Inhibitors, Curr. Pharm. Des., 19 (2013) 1850-1859.

[34] P.A. Kollman, I. Massova, C. Reyes, B. Kuhn, S. Huo, L. Chong, M. Lee, T. Lee, Y. Duan, W. Wang, O. Donini, P. Cieplak, J. Srinivasan, D.A. Case, T.E. Cheatham, Calculating Structures and Free Energies of Complex Molecules: Combining Molecular Mechanics and Continuum Models, Acc. Chem. Res., 33 (2000) 889-897.

[35] H. Pelemans, R. Esnouf, E. De Clercq, J. Balzarini, Mutational Analysis of Trp-229 of Human Immunodeficiency Virus Type 1 Reverse Transcriptase (RT) Identifies This Amino Acid Residue as a Prime Target for the Rational Design of New Non-Nucleoside RT Inhibitors, Mol. Pharmacol., 57 (2000) 954-960.

[36] F. Esposito, C. Sanna, C. Del Vecchio, V. Cannas, A. Venditti, A. Corona, A. Bianco, A.M. Serrilli, L. Guarcini, C. Parolin, M. Ballero, E. Tramontano, Hypericum hircinum L. components as new single-molecule inhibitors of both HIV-1 reverse transcriptase-associated DNA polymerase and ribonuclease H activities, Pathogens and Disease, 68 (2013) 116-124.

[37] A. Corona, F.S. Di Leva, S. Tierry, L. Pescatori, G. Cuzzucoli Crucitti, F. Subra, O. Delelis, F. Esposito, G. Rigogliuso, R. Costi, S. Cosconati, E. Novellino, R. Di Santo, E. Tramontano, Identification of highly conserved residues involved in the inhibition of the HIV-1 ribonuclease H function by diketoacid derivatives, Antimicrob. Agents Chemother., (2014) *In press*.

[38] V. Suchaud, F. Bailly, C. Lion, E. Tramontano, F. Esposito, A. Corona, F. Christ, Z. Debyser, P. Cotelle, Development of a series of 3-hydroxyquinolin-2(1H)-ones as selective inhibitors of HIV-1 reverse transcriptase associated RNase H activity, Bioorg. Med. Chem. Lett., 22 (2012) 3988-3992.

[39] F. Mohamadi, N.G.J. Richards, W.C. Guida, R. Liskamp, M. Lipton, C. Caufield, G. Chang, T. Hendrickson, W.C. Still, Macromodel—an integrated software system for modeling organic and bioorganic molecules using molecular mechanics, J. Comput. Chem., 11 (1990) 440-467.

[40] T. Halgren, Merck molecular force field. II. MMFF94 van der Waals and electrostatic parameters for intermolecular interactions, J. Comput. Chem., 17 (1996) 520-552.

[41] W.C. Still, A. Tempczyk, R.C. Hawley, T. Hendrickson, Semianalytical treatment of solvation for molecular mechanics and dynamics, J. Am. Chem. Soc., 112 (1990) 6127-6129.

[42] Schrödinger LLC., Maestro GUI, in, New York, NY, USA, 2013.

[43] Schrödinger LLC., QMPolarized protocol, in: Schrodinger Suite, New York, NY, USA.

[44] D.Q. McDonald, W.C. Still, AMBER torsional parameters for the peptide backbone, Tetrahedron Lett., 33 (1992) 7743-7746.

[45] PyMOL, in, Molecular Graphics System Schrödinger, LLC.

Table(s)

Table 1. EMAC derivatives effects on the HIV-1 RT-associated functions

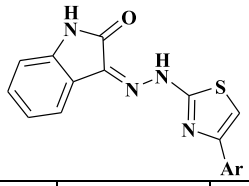

Compound	Ar	RNase H [a]IC_{50} (µM)	DP [b]IC_{50} (µM)	[c]SpI
1		3.2 ± 1.2	0.9 ± 0.3	3.5
EMAC2072		10.6 ± 0.8	20.0 ± 6.0	0.53
EMAC2073		6.4 ± 1.5	23.9 ± 5.7	0.26
EMAC2074		14.9 ± 2.8	81.0 ± 15	0.18
EMAC2075		2.9 ± 0.8	34.0 ± 5	0.08
EMAC2076	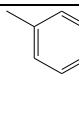	2.5 ± 0.4	22.0 ± 1	0.11
EMAC2077		2.6 ± 0.5	18.5 ± 2.5	0.14
EMAC2078		2.8 ± 0.8	13.0 ± 5	0.21
EMAC2079		9.0 ± 0.9	45.0 ± 2.5	0.20
EMAC2080		4.7 ± 0.5	26.0 ± 5	0.18
EMAC2081		100	71.6 ± 16	1.3
EMAC2082		3.9 ± 1.5	19.5 ± 2.5	0.20
Efavirenz		ND[d]	0.023 ± 0.006	
RDS1643		10.1 ± 2.2	ND	

[a]Compound concentration required to reduce the HIV-1 RT-associated RNase H activity by 50%;
[b]Compound concentration required to reduce the HIV-1 RT-associated RNA-dependent DNA polymerase activity by 50%;
[c]Specificity Index: ratio between compound concentration required to reduce the HIV-1 RT-associated RNase H activity by 50% and compound concentration required to reduce the HIV-1 RT-associated DP activity by 50% (IC_{50} RNase H/IC_{50} DP);
[d]ND, not done.

Table 2: Inhibition of wild-type HIV-1 and the mutants HIV-1 RT associated activities by **EMAC2076** expressed as IC_{50} (□M)

	HIV-1 wt RT		HIV-1 Tyr181Cys RT		HIV-1 Lys103Asn RT	
Compound	**RNase H[a]**	**DP[b]**	**RNase H[a]**	**DP[b]**	**RNase H[a]**	**DP[b]**
EMAC2076	2.5 ± 0.4	22.0 ± 1	2.7 ± 0.8	15.4 ± 2.3	3.42 ± 0.9	18.8 ± 2.7
RDS1643	10.1 ± 2.2	ND[c]	9.6 ± 1.8	ND[c]	9.2 ± 0.9	ND
Efavirenz	ND[c]	0.023 ± 0.006	ND[c]	0.680 ± 0.200	ND	0.280 ± 0.070

[a]Compound concentration required to reduce the HIV-1 RT-associated RNase H activity by 50%
[b]Compound concentration required to reduce the HIV-1 RT-associated RNA-dependent DNA polymerase activity by 50%. [c]ND, not done.

Figure(s)

Figure 1

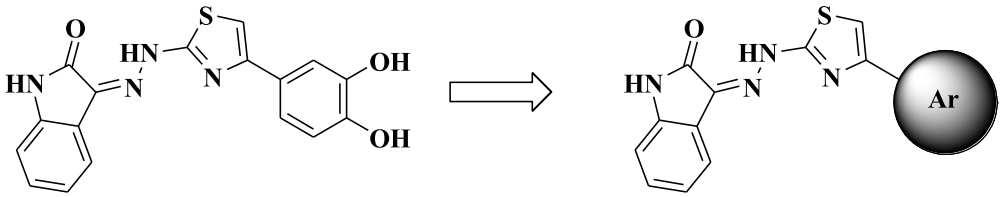

HIT compound 1 EMAC 2072-2082

Scheme 1

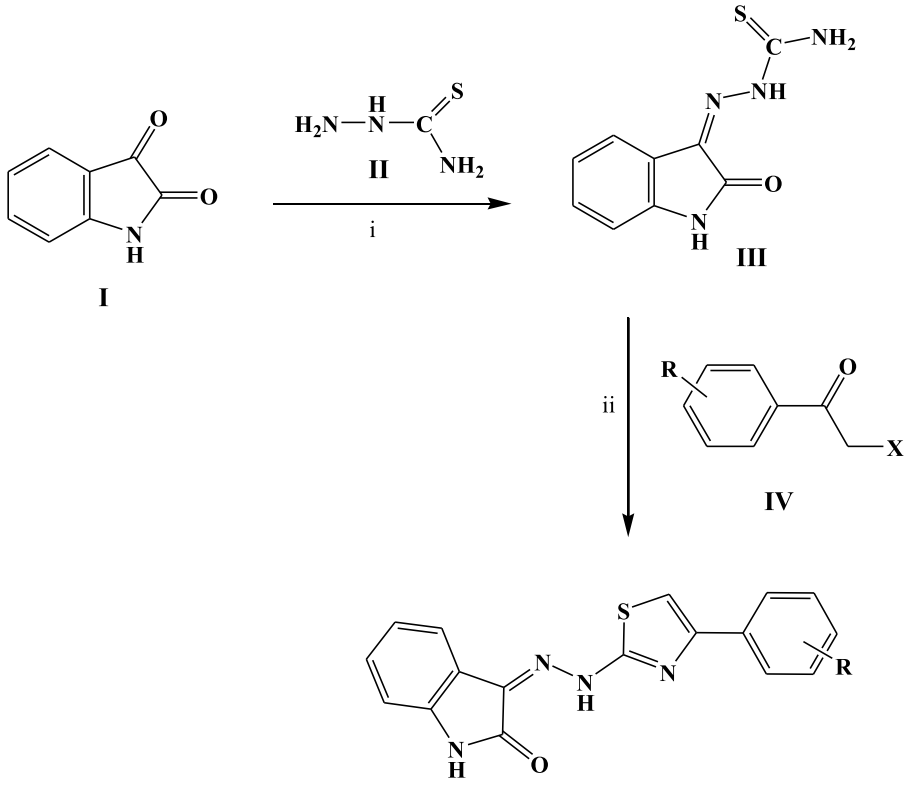

R: 4-Cl, 4-F, 4-Br, 4-NO_2, 4-C_6H_5, 2,4-F, 3-NO_2, 4-CH_3, 4-OCH_3, H, 2,4-Cl

Figure 2

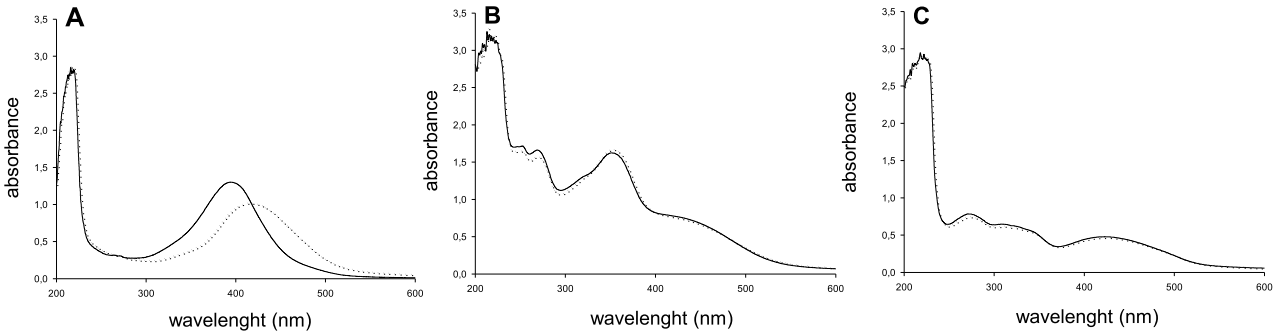
A
B
C
absorbance
wavelenght (nm)
3,5
3,0
2,5
2,0
1,5
1,0
0,5
0,0
200
300
400
500
600

Figure 3

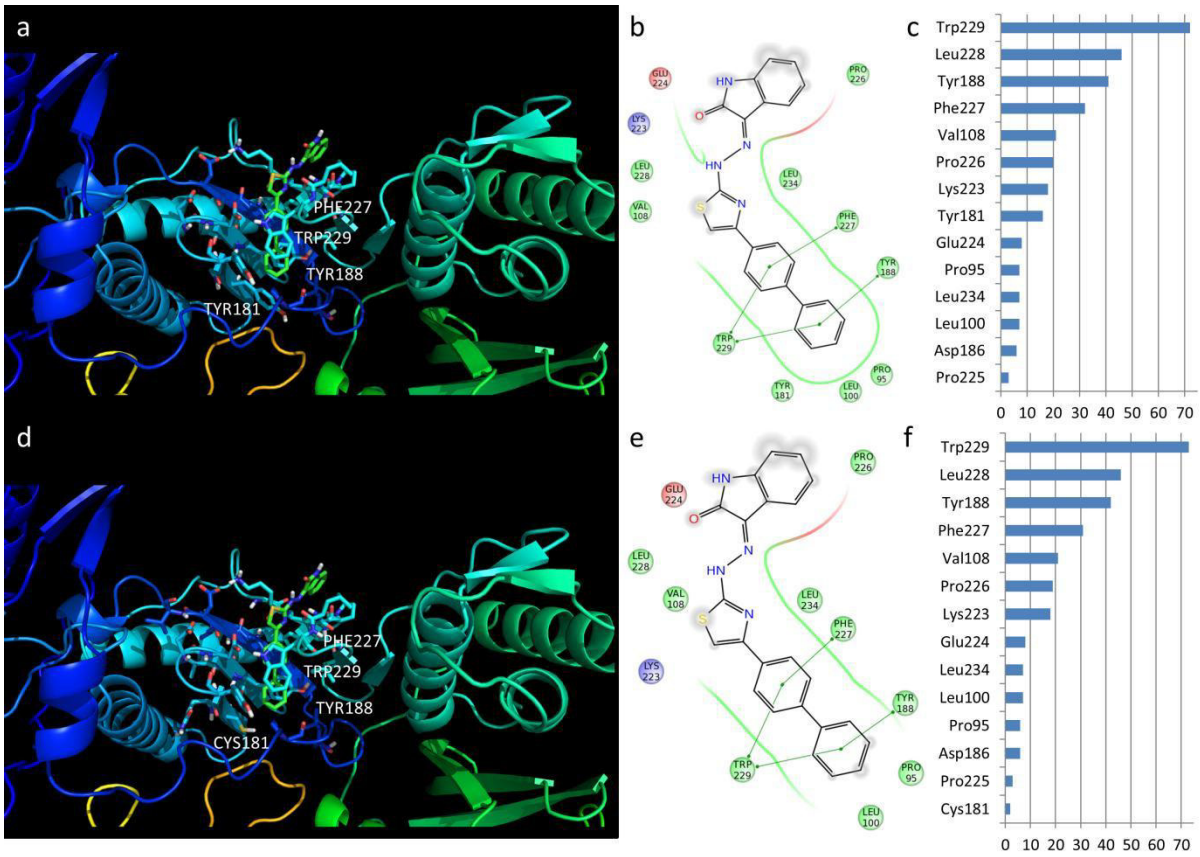
a
PHE227
TRP229
TYR188
TYR181
b
c
Trp229
Leu228
Tyr188
Phe227
Val108
Pro226
Lys223
Tyr181
Glu224
Pro95
Leu234
Leu100
Asp186
Pro225
0 10 20 30 40 50 60 70
d
PHE227
TRP229
TYR188
CYS181
e
f
Trp229
Leu228
Tyr188
Phe227
Val108
Pro226
Lys223
Glu224
Leu234
Leu100
Pro95
Asp186
Pro225
Cys181
0 10 20 30 40 50 60 70

Supplementary Material - For Publication Online

Click here to download Supplementary Material - For Publication Online: EJMC-SD-Meledduetal.docx